DECISION-DIRECTED CHANNEL ESTIMATION FOR MULTI-USER OFDM ENVIRONMENTS

Matthias Münster and Lajos Hanzo[1]

Dept. of Electronics and Computer Science,
University of Southampton, SO17 1BJ, UK.
Tel: +44-1703-593 125, Fax: +44-1703-594 508
Email:lh@ecs.soton.ac.uk
http://www-mobile.ecs.soton.ac.uk

ABSTRACT

Multiple reception antenna assisted Space Division Multiple Access (SDMA) techniques designed for wireless OFDM systems have recently drawn wide interests. These techniques facilitate the implementation of effective multi-user detection algorithms at the receiver, such as Minimum Mean-Square Error (MMSE) detection, Successive Interference Cancellation (SIC), Parallel Interference Cancellation (PIC) or Maximum Likelihood (ML) detection. A prerequisite of their operation is the availability of an estimate of the channel's frequency domain transfer function. Decision-directed channel estimation was analysed by Li *et al.* in the context of a space-time coded single-user arrangement employing two transmit and two receive antennas. This estimation scheme is also applicable to a multi-user scenario, where each user is equipped with a single transmit antenna. The contribution presented here proposes a decision-directed channel estimator, which invokes only subsets of the available subcarriers in order to reduce the interference between the different users' estimation processes.

1. OVERVIEW

In this contribution a decision-directed channel estimator designed for Space Division Multiple Access (SDMA) assisted Orthogonal Frequency Division Multiplexing (OFDM) applications is presented based on a single-user version of the estimator proposed by Li *et al.* in [1]. In our approach only limited subsets of the available subcarriers are employed in the estimation process with the aim of a reducing the effects of the multi-user interference. The structure of the paper is as follows: In Section 2 the SDMA scenario is outlined, followed by a portrayal of Li's estimation scheme [1] in Section 3.1. In Section 3.2 the principles of our approach are described, followed by its performance assessment in Section 4. Our conclusions will be offered in Section 5.

VCT2001 SPRING CONFERENCE, MAY 6-9, 2001, RHODES, GREECE

The financial support of the European Union under the auspices of the Pan-European TRUST project and that of the EPSRC, Swindon UK is gratefully acknowledged

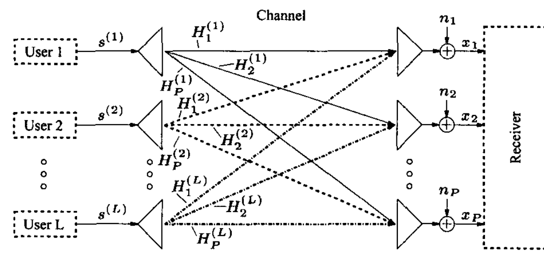

Figure 1: Schematic of an SDMA uplink scenario, where each of the L users is equipped with a single transmit antenna and the receiver is assisted by a P element antenna front-end.

2. THE SIGNAL MODEL

In Figure 1 we have portrayed an SDMA uplink transmission scenario, where each of the P simultaneous users is equipped with a single transmission antenna, while the receiver capitalizes on a P element antenna front-end. The $(P \times 1)$-dimensional vector of complex signals, $\mathbf{x}[n,k]$, received by the P-element antenna array in the k-th subcarrier of the n-th OFDM symbol is constituted by the superposition of the independently faded signals associated with the L users sharing the same space-frequency resource. The received signal was corrupted by the Gaussian noise at the array elements. The indices $[n,k]$ have been omitted for notational convenience during our forthcoming discourse, yielding:

$$\mathbf{x} = \mathbf{H}\mathbf{s} + \mathbf{n}, \qquad (1)$$

where the $(P \times 1)$-dimensional vector $\mathbf{x}$ of received signals, the vector $\mathbf{s}$ of transmitted signals and the array noise vector $\mathbf{n}$, respectively, are given by:

$$\mathbf{x} = (x_1, x_2, \ldots, x_P)^T, \qquad (2)$$

$$\mathbf{s} = (s^{(1)}, s^{(2)}, \ldots, s^{(L)})^T, \quad (3)$$
$$\mathbf{n} = (n_1, n_2, \ldots, n_P)^T. \quad (4)$$

The frequency domain channel transfer function matrix $\mathbf{H}$ of dimension $L \times P$ is constituted by the set of channel vectors of the L users:

$$\mathbf{H} = (\mathbf{H}^{(1)}, \mathbf{H}^{(2)}, \ldots, \mathbf{H}^{(L)}), \quad (5)$$

each of which describes the frequency domain channel transfer function between the single transmitter antenna associated with a particular user l and the reception array elements $p \in \{1, \ldots, P\}$:

$$\mathbf{H}^{(l)} = (H_1^{(l)}, H_2^{(l)}, \ldots, H_P^{(l)})^T, \quad (6)$$

with $l \in \{1, \ldots, L\}$. Regarding the statistical properties of the components associated with the vectors in Equation 1, we assume that the complex data signal $s^{(l)}$ transmitted by the l-th user has zero-mean and unit variance. The AWGN noise process n_p at any antenna array element p exhibits also zero-mean and a variance of σ^2. The frequency domain channel transfer functions $H_p^{(l)}$ of the different array elements $p \in \{1, \ldots, P\}$ or users $l \in \{1, \ldots, L\}$ are independent, stationary, complex Gaussian distributed processes with zero-mean and a different variance of σ_l^2 [2].

3. DESCRIPTION OF THE DECISION-DIRECTED CHANNEL ESTIMATOR

3.1. Motivation

Decision-directed channel estimation has been addressed in a variety of contributions, notably for example the detailed discussions of Li *et al.* in [3] in the context of *single-user* OFDM environments. The basic idea is to equalize the channel transfer function experienced by an OFDM symbol during the current transmission period by capitalizing on the channel information obtained during the previous OFDM symbol period, inherently assuming quasi-invariance of the channel between the two consecutive OFDM symbol transmission intervals. An improved channel estimate can then be obtained for the most recently received OFDM symbol upon dividing the complex symbol received in each subcarrier by the sliced and remodulated information symbol hosted by a subcarrier. The updated channel estimate is then again employed as an initial channel estimate for the next OFDM symbol transmission period.

By contrast, in the multi-user OFDM scenario outlined in Section 2 the signal received by each antenna is constituted by a superposition of the signal contributions associated with the different users, as given by Equation 1. Hence, an estimate of the channel between the single transmission antenna of a specific user and any of the receiver antennas at the basestation *cannot* be inferred using the same strategy as in the single user case. In [1,4] a Minimum Mean-Square Error (MMSE) approach was discussed, which aims at obtaining the estimates $\hat{H}_p^{(l)}[n,k]$ of the different channel transfer factors by minimizing the aggregate squared differences between the complex symbols $x_p[n,k]$ actually received and the estimates $\hat{x}_p[n,k]$, $k \in \{0, \ldots, K-1\}$, separately for each reception branch $p \in \{1, \ldots, P\}$. This is reflected by the following cost-function, where the index p of the reception antenna and the index n associated with the OFDM symbol period have been omitted for notational convenience [1]:

$$C = \sum_{k=0}^{K-1} |x[k] - \hat{x}[k]|^2, \quad (7)$$

where $\hat{x}[k]$ is given by [1]:

$$\hat{x}[k] = \sum_{l=1}^{L} \hat{H}^{(l)}[k] s^{(l)}[k], \quad (8)$$

assuming knowledge of the transmitted symbols $s^{(l)}[k]$. In order to render the estimation problem tractable it is beneficial to represent each channel transfer factor $\hat{H}^{(l)}[k]$ by the Fourier Transform (FT) of the corresponding CIR tap estimates $\hat{h}^{(l)}[\acute{n}]$, $\acute{n} \in \{0, \ldots, K_0 - 1\}$ [1]:

$$\hat{H}^{(l)}[k] = \sum_{\acute{n}=0}^{K_0-1} \hat{h}^{(l)}[\acute{n}] W_K^{k\acute{n}}, \quad (9)$$

where $W_K = \exp(-j2\pi/K)$ is the complex Fourier kernel. Consequently the task is to find estimates $\hat{h}^{(l)}[\acute{n}]$ for the CIR taps under the constraint of minimising the costfunction C in Equation 7, which can be achieved upon invoking standard optimization techniques. In [1,4] Li *et al.* demonstrated that the estimator exhibits the optimum MSE performance, if the symbol sequences $s^{(1)}[k]$ and $s^{(2)}[k]$ transmitted by the two antennas in a specific OFDM symbol period are related such that the estimation processes of the different CIR taps are decoupled. In [1] this condition was given by:

$$s^{(2)}[k] = (-1)^k s^{(1)}[k], \quad (10)$$

while in [4] the same principle was extended to an M-antenna system leading to:

$$s^{(i)}[k] = s^{(1)}[k] W_K^{-\bar{K}_0(i-1)k}, \quad (11)$$

where $\bar{K}_0 = \lfloor \frac{K}{M} \rfloor \geq K_0$ and $\lfloor x \rfloor$ denotes the largest integer smaller than or equal to x. Since this condition does not normally hold for arbitrary data symbols, a sufficiently high number of subcarriers is required to reduce the cross-correlation between the different users' transmitted symbol sequences. In the next section we will highlight our approach to the problem of decision-directed channel estimation.

3.2. Concept of the Enhanced Estimator

In [6] orthogonal Walsh-coded periodic pilot patterns were employed in order to allow for a separation of the channel transfer functions between the different transmit and receive antennas in an SDMA scenario. The basic idea was to assign a unique M-chip Walsh coded reference vector $\mathbf{r}^{(l)} = (r_0^{(l)}, r_1^{(l)}, \ldots, r_{M-1}^{(l)})$ with $r_i^l \in \{1, -1\}\ \forall\ i \in \{0, \ldots, M-1\}$ to each of the L users. Instead of employing only one regularly-spaced pilot grid for sampling the channel's transfer function, as in the single-user scenario, M

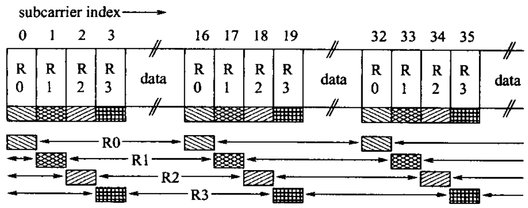

Figure 2: Pilot arrangement in each OFDM symbol of the system proposed in [6]; a *reference length of* $M = 4$ *bits* and an *intra-group pilot distance of* 16 *subcarriers* is assumed; interpolation is performed between the 16-subcarrier-spaced pilots associated with the same grid position within the reference sequence.

parallel pilot grids were employed. Each of the M grids was assigned to a specific element of the M-chip reference vector. To be more explicit, all of the L users were instructed to transmit the i-th element of their M-chip reference vector in all regularly-spaced pilot subcarriers associated with the i-th pilot grid. At the receiver the different reference pilot grids were interpolated separately - also for different reception antennas - by means of DFT-based low-pass interpolation. More explicitly, the complex channel transfer factor of each subcarrier of the different users was then extracted upon arranging the regularly-spaced pilot grid estimates in a column-vector, followed by the evaluation of its inner product with the user's orthogonal reference vectors $\mathbf{r}^{(l)}$. The result was then normalised to the number of elements M hosted by the reference vector. These concepts are further illustrated in Figure 2 for $M = 4$ and an intra-group pilot distance of 16 subcarriers [6].

However, in the context of the decision-directed channel estimator considered here, no pilots are explicitly transmitted during data OFDM symbol periods. Instead, all the sliced and remodulated data symbols can be viewed as 'pilot' information in the absence of transmission errors. Commencing with the basic scenario of two simultaneous BPSK-modulated users, each subcarrier is associated with one out of a set of 4 possible BPSK symbol combination vectors $(b^{(0)}, b^{(1)})$, namely S={(1,1),(1,-1),(-1,1),(-1,-1)}. This set can be divided into two subsets, namely $S^I = \{(1,1),(1,-1)\}$, $S^{II} = \{(-1,-1),(-1,1)\}$ of linearly independent row vectors, where $S^I \bigcup S^{II} = S$ and $S^I \bigcap S^{II} = \emptyset$. Both S^I and S^{II} constitute a basis for a two-dimensional vector space. Hence the task is to relate the Symbol Combination Vector (SCV) associated with each subcarrier to one of the elements contained in S^I or S^{II}. Each basis vector contained in S^{II} corresponds to a co-linear basis vector contained in S^I and vice versa, where the co-linear basis vectors are related to each other by a scalar constant of -1. Those complex subcarrier symbols, whose SCV is associated with one of the elements from S^{II} can hence be multiplied with the scalar constant of -1, so that their SCV becomes associated with S^I instead of S^{II}. Following the same steps as in the case of the Walsh-coded pilot reference sequences [6] described above, MMSE interpolation is performed separately between the subcarriers

f_s	f_c	N_{path}	$RMS(\tau)$
225MHz	60GHz	3	$16.9ns$
FFT length	cycl. prefix	$f_{d,max}$	$f'_{d,max}$
512	64	2778Hz	$1.235 * 10^{-5}$

Table 1: Parameters of the indoor WATM environment [5].

associated with each of the basis vectors contained in S^I, upon invoking a single-user version of Li's MMSE estimator, which was outlined in Section 3.1. The extraction of the different channel transfer factors can then be achieved for each subcarrier upon evaluating the inner product between the vector hosting the interpolated channel transfer factors associated with the basis vectors in this subcarrier and the basis vectors itself, again followed by normalization.

In terms of bandwidth efficiency employing BPSK is not the most favourable option. Hence we also examine, whether the same principles can be applied to QPSK modulation, as it was also studied in [1–4]. In a QPSK modulated system supporting two simultaneous users the set S of SCVs potentially hosts 16 entries. In accordance with our procedure proposed for BPSK, the set S can be separated into 4 subsets hosting 4 SCVs each, satisfying $S^I \bigcup S^{II} \bigcup S^{III} \bigcup S^{IV} = S$ and $S^I \bigcap S^{II} \bigcap S^{III} \bigcap S^{IV} = \emptyset$. Again, as a result of the rotational invariance properties of the QPSK modulation scheme, each set S^x can be transformed into every other set S^y, $x, y \in \{I, II, III, IV\}$ upon multiplication by a complex constant. $S^{(I)}$ could be for example $\{(1,1),(1,-1),(1,j),(1,-j)\}$. It should be noted that any vector $s^x \in S^i$ is linearly independent from any other single vector $s^y \in S^I \setminus s^x$ and hence s^x, s^y form a basis for a two-dimensional vector space and are therefore capable of recovering the complex channel transfer factors of each subcarrier. The set S^I of SCVs can be split into two subsets of basis vectors $S_1^I = \{(1,1),(1,-1)\}$ and $S_2^I = \{(1,j),(1,-j)\}$ with $S_1^I \bigcup S_2^I = S^I$ and $S_1^I \bigcap S_2^I = \emptyset$, which simplifies the extraction of the channel transfer factors. Since both sets form a basis of the desired vector space, it would be sufficient to select only the subcarriers associated with either the first or the second set for interpolation. By contrast, upon averaging the channel estimates obtained for both sets of basis vectors a further $3dB$ reduction of the channel estimator's MSE was achieved as it will be shown in Section 4. Here we considered the case of two simultaneous users- or transmit antennas as in [1]. The proposed scheme could potentially be further extended for a scenario of for example 4 simultaneous QPSK modulated users.

4. SIMULATION RESULTS

Simulations were conducted for an SDMA uplink scenario supporting two simultaneous OFDM users equipped with one transmit antenna each. At the basestation (BS) two reception antennas were assumed, where each of the independently faded channels is characterized by the parameters of the indoor WATM channel environment given in Table 1 [5]. We considered 'frame-invariant' fading, where the fading envelope has been keept constant during each OFDM symbol's transmission period. This avoided the ob-

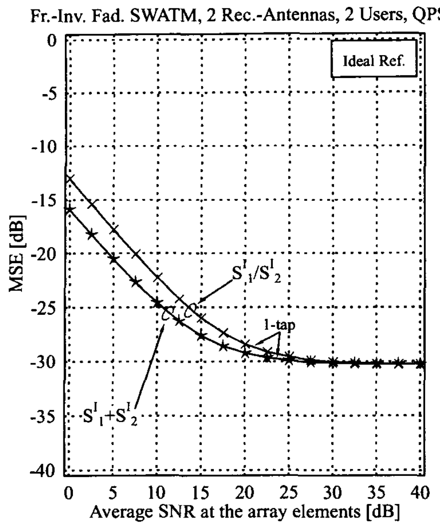

Figure 3: Channel estimation MSE performance (σ^2=2) of the estimator capitalizing on one set of remodulated subcarriers ('S_1^I/S_2^I'), and the estimator invoking both sets of remodulated subcarriers ('$S_1^I + S_2^I$'), further assisted by 1-tap time-domain CIR-tap prediction and upon stipulating an *ideal, error-free reference signal*; each of the SDMA scenario's independently faded channels is characterized by the indoor WATM channel parameters of Table 1 [5]; the maximum path delay resolved by the CIR estimator was 11 taps.

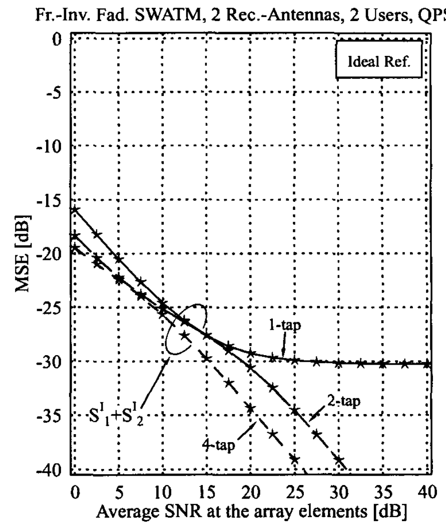

Figure 4: Channel estimation MSE performance (σ^2=2) of the estimator invoking both sets of remodulated subcarriers ('$S_1^I + S_2^I$'), further assisted by 1, 2 or 4-tap time-domain CIR-tap prediction and upon stipulating an *ideal, error-free reference signal*; each of the SDMA scenario's independently faded channels is characterized by the indoor WATM channel parameters of Table 1 [5]; the maximum path delay resolved by the estimator was 11 taps.

fuscating effects of inter-subcarrier interference and hence will enable us to study the various channel estimation effects in isolation. In Figure 3 we have portrayed the MSE exhibited by the different channel impulse response (CIR) estimation schemes without the assistence of channel prediction. At sufficiently high SNRs a residual channel estimation MSE of about $-30dB$ is observed for the channel estimators proposed in this contribution. Specifically, the estimator 'S_1^I/S_2^I' employed only one of the two available SCV subsets, while ' $S_1^I + S_2^I$' performed an averaging of the channel estimates obtained from the two SCV subsets S_1^I and S_2^I. For lower channel SNRs the estimator '$S_1^I + S_2^I$' capitalizing on both subcarrier sets outperforms the estimator relying on only one set by about 3dB in terms of the MSE. This is a result of the noise mitigation achieved by averaging over the imperfect channel estimates delivered independently by the two sets of subcarriers. As seen in Figure 3, the MSE exhibits a residual floor. This is due to the evolution of the channel's frequency-domain transfer function between successive OFDM symbols.

In order to further reduce the residual MSE observed in conjunction with the different CIR estimation schemes, N-tap time-domain MMSE CIR-tap prediction filtering can be employed [3, 12]. The corresponding channel estimator MSE results are portrayed in Figure 4. In the context of the relatively slowly fading WATM channel of Table 1 assumed here, where the residual MSE is observed due to the channel transfer function's evolution, rather than due to the imperfections of the channel estimator, both the two- and four-tap CIR-tap prediction filters succeed in substantially reducing the residual MSE, as illustrated in Figure 4. Hence, in our further simulations we employed four-tap CIR-tap prediction.

In order to further assess the channel estimation accuracy we have studied an OFDM receiver structure incorporating the different estimation approaches in conjunction with MMSE antenna combining [2, 6, 7] or SIC [7–9]. The BER simulation results are illustrated in Figure 5. To be more realistic, in contrast to the simulations conducted in the context of Figures 3 and 4 we have employed the potentially error contaminated, remodulated output signal of the demodulator as a reference signal in the process of decision-directed channel estimation. We observe that the proposed estimator does not encounter a residual BER in the considered range of SNRs. Furthermore, we observe that among the two estimators, the approach ' $S_1^I + S_2^I$' capitalizing on both sets of subcarriers only provides a slightly improved performance. A similar BER as portrayed in Figure 5 was also observed in the context of a system incorporating Li's original channel estimator.

5. CONCLUSIONS

In this contribution we have presented a decision-directed channel estimator applicable to multi-user SDMA OFDM

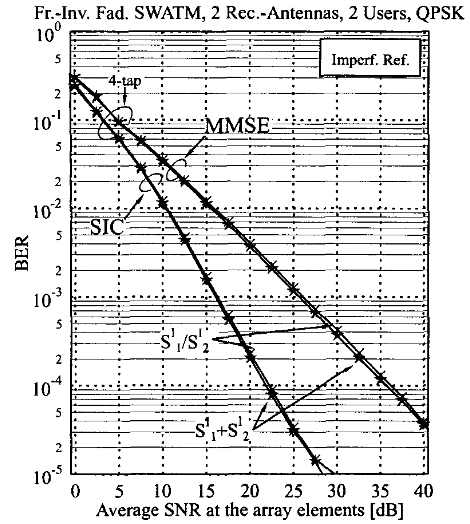

Figure 5: BER performance of the estimator capitalizing on one set of remodulated subcarriers ('S_1^I/S_2^I'), and the estimator invoking both sets of remodulated subcarriers ('$S_1^I + S_2^I$'), further assisted by 4-tap time-domain CIR-tap prediction and using a *potentially error-contaminated reference signal*; each of the SDMA scenario's independently faded channels is characterized by the indoor WATM channel parameters of Table 1 [5]; the maximum path delay resolved by the estimator was 11 taps; two detection techniques, namely MMSE combining or SIC were employed; training information was assigned to every 16-th OFDM symbol in order to suppress error propagation between successive OFDM symbols.

environments or, alternatively, to single-user space-time coded scenarios involving multiple transmit antennas. Here we focussed our attention on the case of two simultaneous QPSK users, but the concepts invoked can be potentially extended to scenarios supporting a higher number of users.

6. REFERENCES

[1] Y. Li, N. Seshadri, and S. Ariyavisitakul, "Channel Estimation for OFDM Systems with Transmitter Diversity in Mobile Wireless Channels," *IEEE Journal on Selected Areas in Communications*, vol. 17, pp. 461–471, March 1999.

[2] Y. Li and N. R. Sollenberger, "Adaptive Antenna Arrays for OFDM Systems with Cochannel Interference," *IEEE Transactions on Communications*, vol. 47, pp. 217–229, Feb 1999.

[3] Y. Li, L. J. Cimini, and N. R. Sollenberger, "Robust Channel Estimation for OFDM Systems with Rapid Dispersive Fading Channels," *IEEE Transactions on Communications*, vol. 46, pp. 902–915, Apr 1998.

[4] Y. Li, "Optimum Training Sequences for OFDM Systems with Multiple Transmit Antennas," in *Proc. of Global Telecommunications Conference - Globecom'00*, vol. 3, (San Francisco, California), pp. 1478–1482, IEEE, November 27 - December 1 2000.

[5] L. Hanzo, W. Webb, and T. Keller, *Single- and Multi-carrier Quadrature Amplitude Modulation.* IEEE Press- John Wiley, April 2000.

[6] M. Münster, T. Keller, and L. Hanzo, "Co–Channel Interference Suppression Assisted Adaptive OFDM in Interference Limited Environments," in *Proc. of Vehicular Technology Conference*, vol. 1, (Amsterdam, Netherlands), pp. 284–288, IEEE, September 19-22 1999.

[7] P. Vandenameele, L. V. der Perre, M. Engels, and H. D. Man, "A Novel Class of Uplink OFDM/SDMA Algorithms for WLAN," in *Proc. of Global Telecommunications Conference - Globecom'99*, vol. 1, (Rio de Janeiro, Brazil), pp. 6–10, IEEE, December 5-9 1999.

[8] G. D. Golden, G. J. Foschini, R. A. Valenzuela, and P. W. Wolniansky, "Detection Algorithms and Initial Laboratory Results using V-BLAST Space-Time Communication Architecture," *IEE Electronics Letters*, vol. 35, pp. 14–16, Jan. 1999.

[9] M. Münster and L. Hanzo, "Co-Channel Interference Cancellation Techniques for Antenna Array Assisted Multiuser OFDM Systems," in *Proc. of 3G-'2000 Conference*, vol. 1, (London, Great Britain), pp. 256–260, IEE, March 27-29 2000.

[10] G. Awater, A. v. Zelst, and R. v. Nee, "Reduced Complexity Space Division Multiplexing Receivers," in *Proc. of Vehicular Technology Conference*, vol. 1, (Tokyo, Japan), pp. 11–15, IEEE, May 15-18 2000.

[11] M. Speth, A. Senst, and H. Meyr, "Low Complexity Space-Frequency MLSE for Multi-User COFDM," in *Proc. of Global Telecommunications Conference - Globecom'99*, vol. 1, (Rio de Janeiro, Brazil), pp. 2395–2399, IEEE, December 5-9 1999.

[12] A. Duel-Hallen, S. Hu, and H. Hallen, "Long Range Prediction of Fading Signals," *IEEE Signal Processing Magazine*, vol. 17, pp. 62–75, May 2000.